Coherent Nonlinear Optical Propagation Processes in Hyperbolic Metamaterials

Alexander Popov
Purdue University, Birck Nanotechnology Center
popov@purdue.edu , https://nanohub.org/groups/nlo/popov

- Coherence and interference in nonlinear and quantum optics;
- Metamaterials and backward light;
- Extraordinary coherent nonlinear optics with backward light.

Coherent Effects in Phsics and Chemistry
Purdue Quantum Center Workshop • Purdue University, West Lafayette, IN • 28 April 2017

Coherent Control

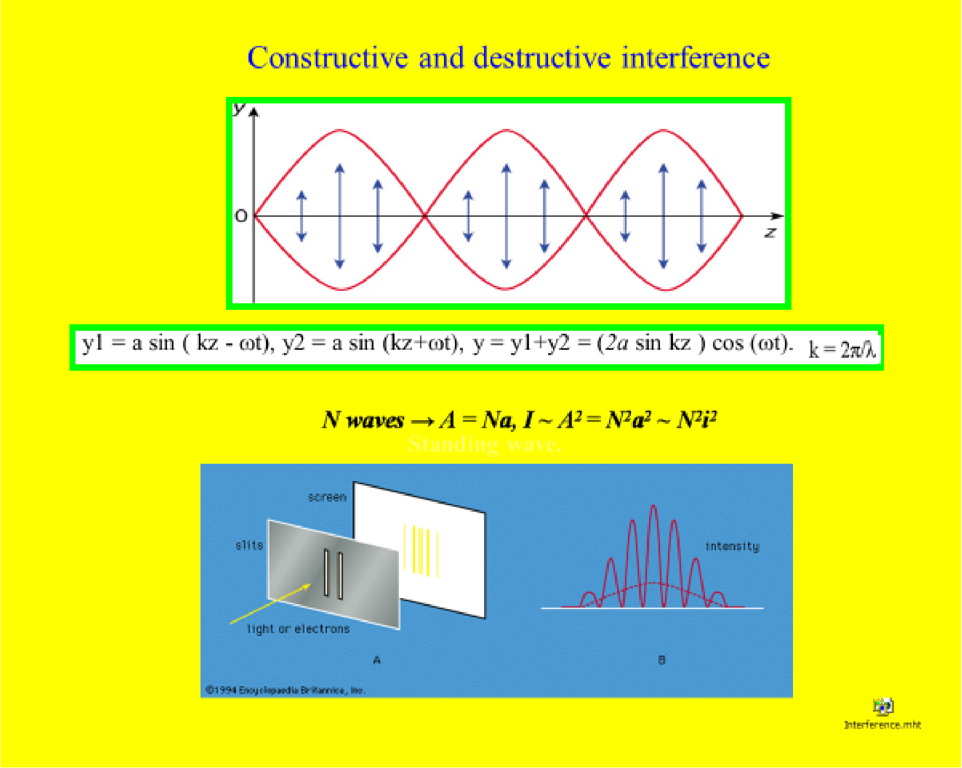

$$P(t) = \chi^{L} E_p(t) + \chi^{(3)} |E(t)|^{2} E_p(t)$$

Interference of Quantum Pathways
Coherent Quantum Control:
Laser Induced Resonances in the Absorption and Refraction Indices, Amplification without Inversion

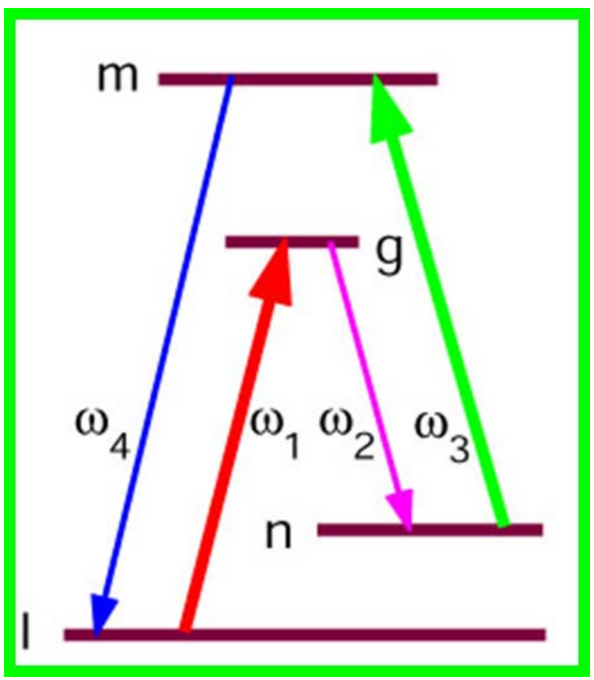

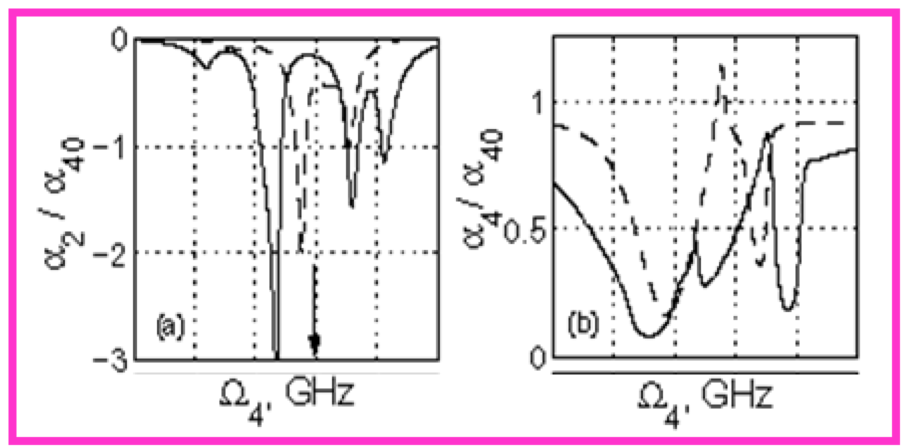

Laser-induced Fano Resonance - Laser Induced Continuum Structures

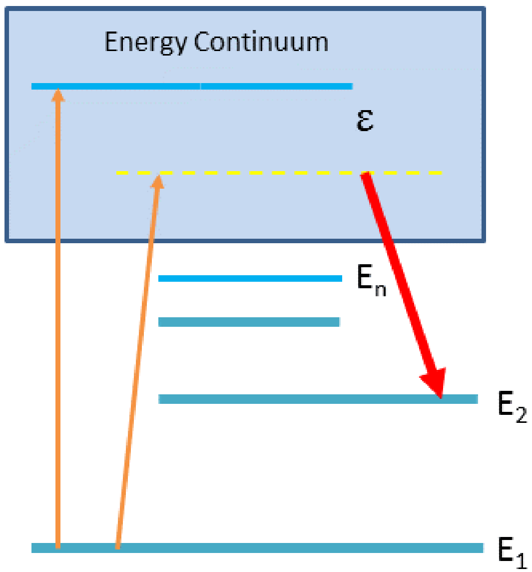

Laser-induced Fano Resonance -
Lase-induced Continuum Structures (LICS)

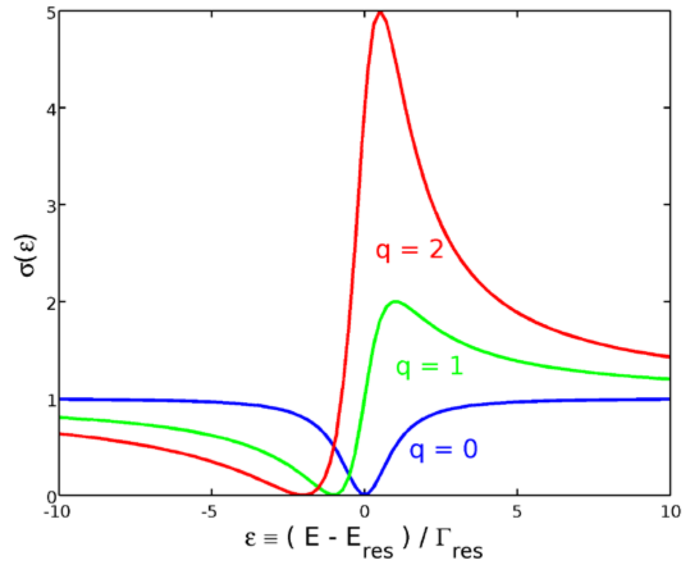

Fano Resonance

Similar Applications to Metamaterial Engineering and Nanophotonics.

Propagation of Light: Phase Velocity, Refractive Index and Poynting Vector

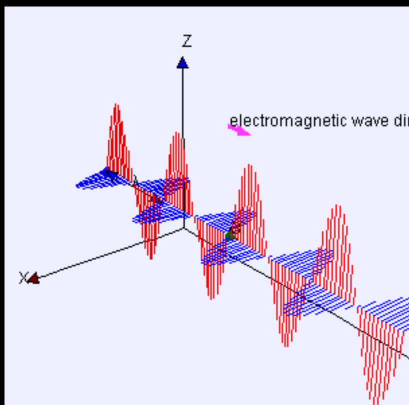

$$\vec{E} = \vec{E}_0 \exp\{i(\omega t - \vec{k}\,\vec{r})\}$$

$$k = n\frac{\omega}{c}$$

$\omega t - kr = 0$; $r/t = v_{ph} = \omega/k = c/n$;
$k = n\,\omega/c$; $n = c/v_{ph} = (\varepsilon\mu)^{1/2}$.

Silicon, 1200 – 8500 nm, n=3.42–3.48;
Germanium, 3000 – 16000 nm, n=4.05–4.01

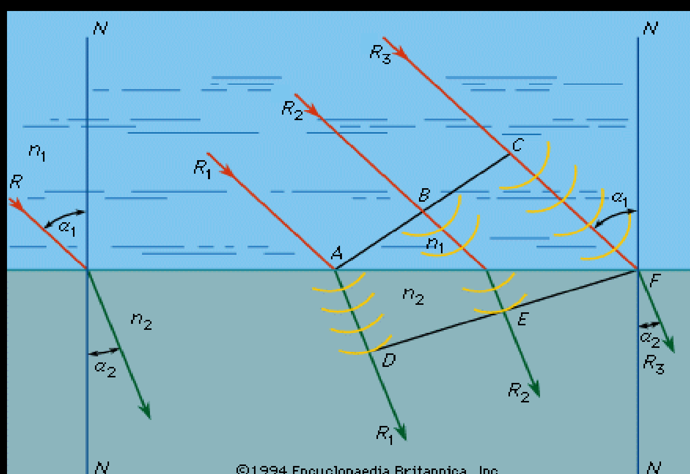

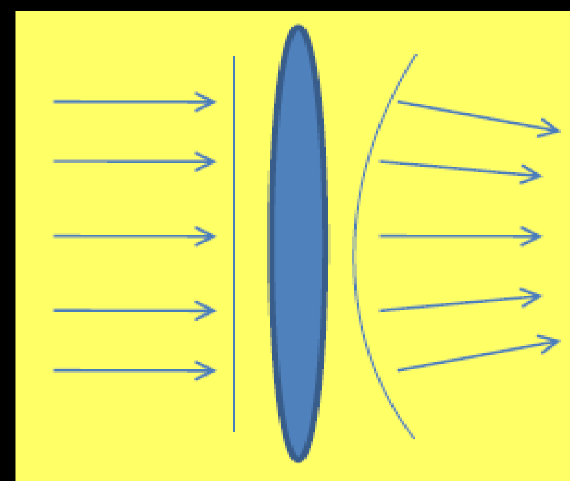

Phase and wave front control

$$\vec{S} = \frac{c}{4\pi}\vec{E}\times\vec{H} = \frac{c^2\vec{k}}{4\pi\omega\varepsilon}H^2 = \frac{c^2\vec{k}}{4\pi\omega\mu}E^2$$

Energy Flux

Nonlinear Optics (Nonlinear Photonics)

$$P(t, z) = P^{L}(t, z) + P^{NL}(t, z);$$

$$P^{L}(t, z) = \chi^{(L)} E(t,z) \; ; \; P^{NL}(t, z) = \chi^{(2)} E^{2}(t,z) + \chi^{(3)} E^{3}(t,z) + \ldots;$$

$$E(t,z) = \Sigma_j E_{0j} \cos(\omega_j t - k_j z) \; ;$$

$$P^{(2)}(t,z) = \Sigma_{i,j} \chi^{(2)} E_{oi} E_{oj} \cos(\omega_i t - k_i z) \cos(\omega_j t - k_j z);$$

$$P^{(3)}(t,z) = \Sigma_{i,jl} \chi^{(3)} E_{oi} E_{oj} E_{ol} \cos(\omega_i t - k_i z) \cos(\omega_j t - k_j z) \cos(\omega_l t - k_l z).$$

Second order, quadratic nonlinearity – SHG, three-wave mixing:

- $\chi^{(2)} \longrightarrow$ $\cos(x)^2 = (1/2)[1+\cos 2x] \longrightarrow 2\omega_i$,
- $\chi^{(2)} \longrightarrow$ $\cos(x)\cos(y) = (1/2)[\cos(x+y)+\cos(x-y)] \longrightarrow$

$$\omega_i + \omega_j = \omega_l \,, \;\; \omega_l - \omega_j = \omega_i \; ;$$

Third order, cubic nonlinearity - THG, four-wave mixing:

- $\chi^{(3)} \longrightarrow$ $\cos^3 x = ¼\,(3\cos x + \cos 3x) \longrightarrow \omega_i \,, 3\omega_i \,,$
- $\chi^{(3)} \longrightarrow \omega_s = \omega_i \quad \omega_j \quad \omega_l \,, \;\; \omega_i + \omega_j = \omega_l + \omega_s,$

Medium Polarization – Linear and Nonlinear

$E(t,z) = E_0 \exp(\omega t - kz);$

$P(t,z) = Nd(t,z) = P^L(t, z) + P^{NL}(t, z)$; $P^L(t, z) = \chi^{(L)} E(t,z);$

$P^{NL}(t, z) = \chi^{(2)} E^2(t,z) + \chi^{(3)} E^3(t,z) + \ldots;$

$P^{(2)}(t,z) = \chi^{(2)} E_o^{\,2} \exp[2\omega t - 2k(\omega)z] \rightarrow$

$E_2(t,z) = E_0 \exp[2\omega t - k(2\omega)z];$

Phase matching: $\Delta k = 2k(\omega) - k(2\omega) = 0 \rightarrow n(\omega) = n(2\omega).$

$E(t,z) = E_3 \exp(\omega_3 t - k_3 z) + E_2 \exp(\omega_2 t - k_2 z);$

$\omega_1 = \omega_3 - \omega_2;\ \ \hbar\omega_3 \rightarrow \hbar\omega_2 + \hbar\omega_1$: OPA and DFG

Phase matching: $k_3 - k_2 = k_1;\ \Delta k = k_3 - k_2 - k_1;\ L_{coh} \sim \pi/\Delta k.$

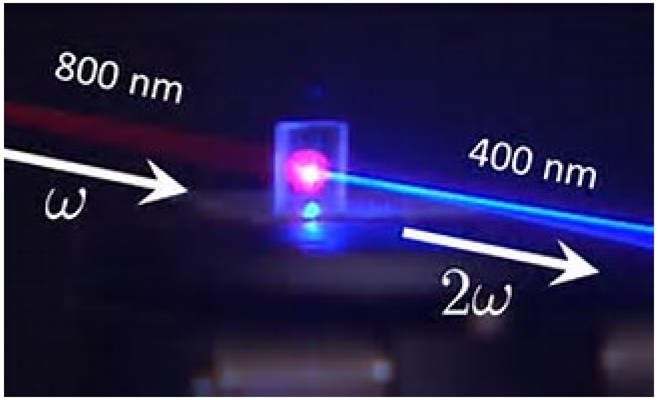

Second Harmonic Generation Phase Matching

$$\frac{\partial E(2\omega)}{\partial z} = -\frac{i\omega}{n_{2\omega}c} d_{\text{eff}} E^2(\omega) e^{i\Delta k z}$$

where $\Delta k = k(2\omega) - 2k(\omega)$.

$$I(2\omega, l) = \frac{2\omega^2 d_{\text{eff}}^2 l^2}{n_{2\omega} n_\omega^2 c^3 \epsilon_0} \left(\frac{\sin(\Delta k l/2)}{\Delta k l/2} \right)^2 I^2(\omega), \quad l_c = \frac{\pi}{\Delta k}$$

Phase dependent (coherent) NLO effects.

Forward and Backward Waves

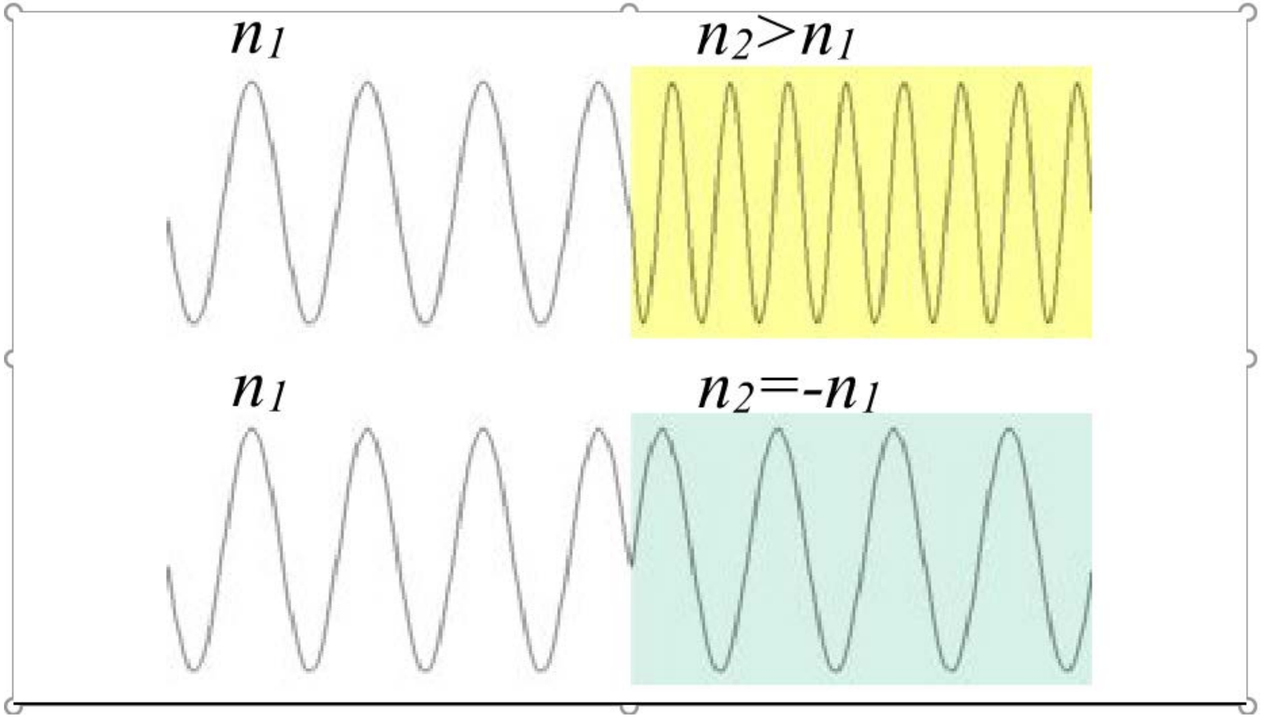

Backward EM waves: striking changes in linear and nonlinear optics

V. Veselago J. Pendry D. Smith V. Shalaev

PIM, FW

NIM, BW

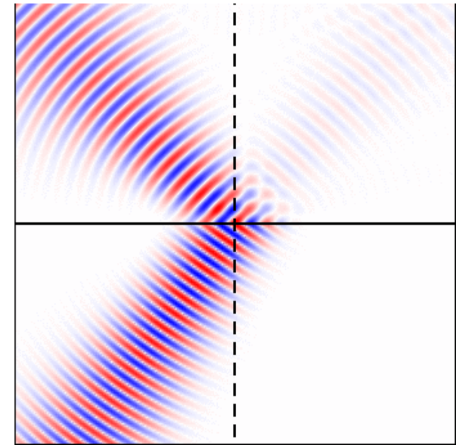

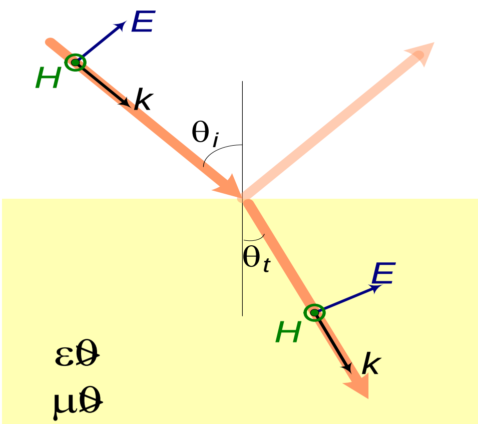

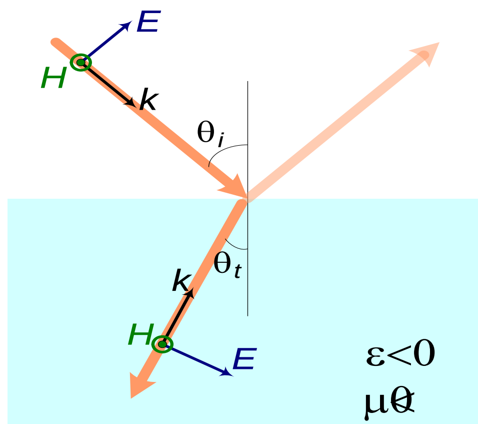

$$\vec{S} = \frac{c}{4\pi}\vec{E}\times\vec{H} = \frac{c^2\vec{k}}{4\pi\omega\varepsilon}H^2 = \frac{c^2\vec{k}}{4\pi\omega\mu}E^2$$

$\mu < 0$, $\varepsilon<0$; $n=-(\varepsilon\mu)^{1/2}$

Negative Refraction:

$$\vec{E}=\vec{E}_0\exp\{i(\omega t-\vec{k}\,\vec{r})\}$$

$$k = n\frac{\omega}{c}$$

PIM, FW **NIM, BW**

Nanoscopic LC ciruits

W. Cai and V. Shalaev, Optical Metamaterials: Fundamentals and Applications, Springer, 2009;
https://engineering.purdue.edu/~shalaev/

SHG: CW REGIME

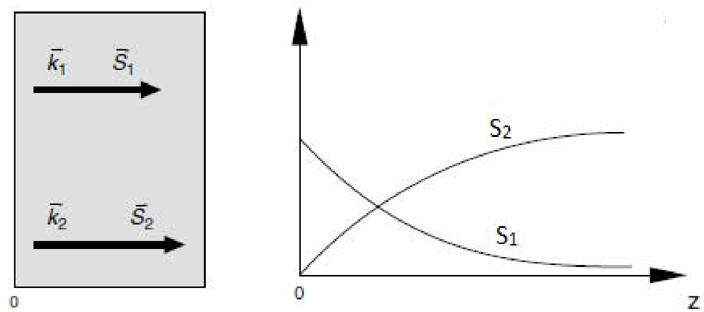

SHG in Ordinary Medium

$$s_2 da_2/dz = -iga_1^2, \quad s_1 da_1/dz = -i2g^* a_1^* a_2.$$

$$2|a_2|^2 + |a_1|^2 = 1.$$

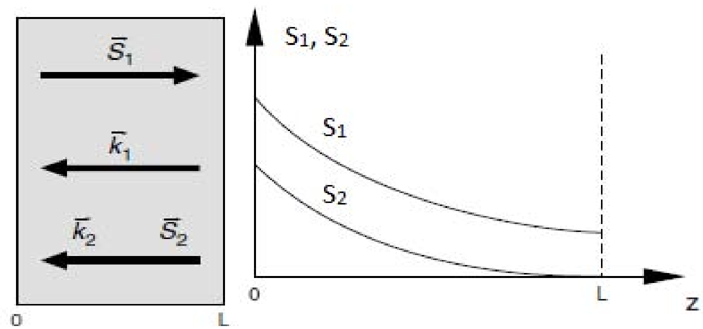

SHG in a Backward Wave Medium

$$da_2/dz = -iga_1^2, \quad da_1/dz = i2g^* a_1^* a_2.$$

$$|a_1|^2 - 2|a_2|^2 = |B|^2 \qquad B = \cos\left(B\sqrt{2}gL\right).$$

Frequency-doubling NLO metamirror

Popov, Slabko, Shalaev, Laser Phys. Lett. **3**, 293-296 (2006).
Popov, Shalaev, Appl. Phys. B Lasers Opt. **84**, 131- 137 (2006).
Shadrivov, Zharov, Kivshar, JOSA B23, 529-534 (2006).
Kudyshev, Gabitov, Maimistov, PRA **87**, 063840 (2013).

Contra-propagating SH Inside the Travelling Pulse of Fundamental Radiation

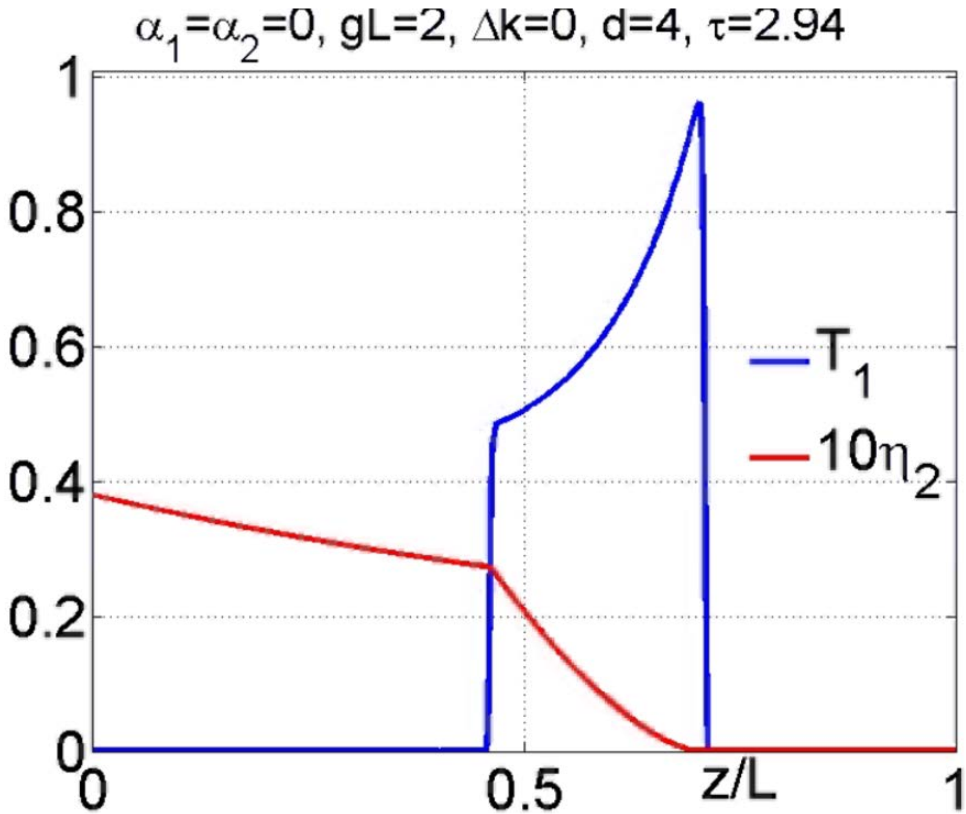

Extraordinary Three-wave Mixing

Ordinary waves

RHM

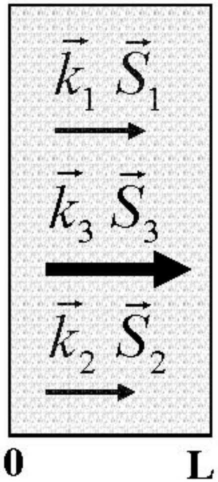

$$P_1^{NL} = \chi_{e1}^{(2)} E_3 E_2^* \exp\{i[(k_3 - k_2)z - \omega_1 t]\},$$
$$P_2^{NL} = \chi_{e2}^{(2)} E_3 E_1^* \exp\{i[(k_3 - k_1)z - \omega_2 t]\},$$

$\boxed{\omega_3 - \omega_1 = \omega_2}$ $\boxed{\omega_3 - \omega_2 = \omega_1}$

$\boxed{\vec{k}_3 - \vec{k}_1 = \vec{k}_2}$ $\boxed{\vec{k}_3 - \vec{k}_2 = \vec{k}_1}$

$\boxed{\hbar\omega_3 = \hbar\omega_1 + \hbar\omega_2}$ $\boxed{\vec{k}_1 + \vec{k}_2 = \vec{k}_3}$

ω_1- signal ω_2 - idler

Entangled Photons

Backward wave

LHM

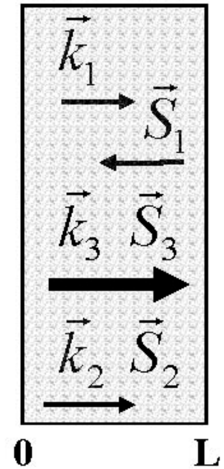

$S_{1,2} \propto \exp(gz)$ $g \propto \chi^{(2)} E_3$ **z = 0,** **$S_{1,2} \propto 1/\cos^2(gL)$**

gL → π/2 – extraordinary resonance, *mirrorless* OP oscillation threshold, huge enhancement in parametric amplification and frequency-shifted NLO reflectivity, propagation direction control, contra-propagating entangle photons.

Popov, Shalaev, *Appl. Phys. B*. 84, 131–137 (2006).
Popov, Shalaev, *Opt.Lett*. 31, 2169–2171 (2006);

Extraordinary transient processes in the pulsed regimes.

Extraordinary applications. Key requirements: BW and FWs, phase matching.

Remotely interrogated nonlinear-optical sensors

$\chi^{(2)}$

$k_1 + k_2 = k_3$

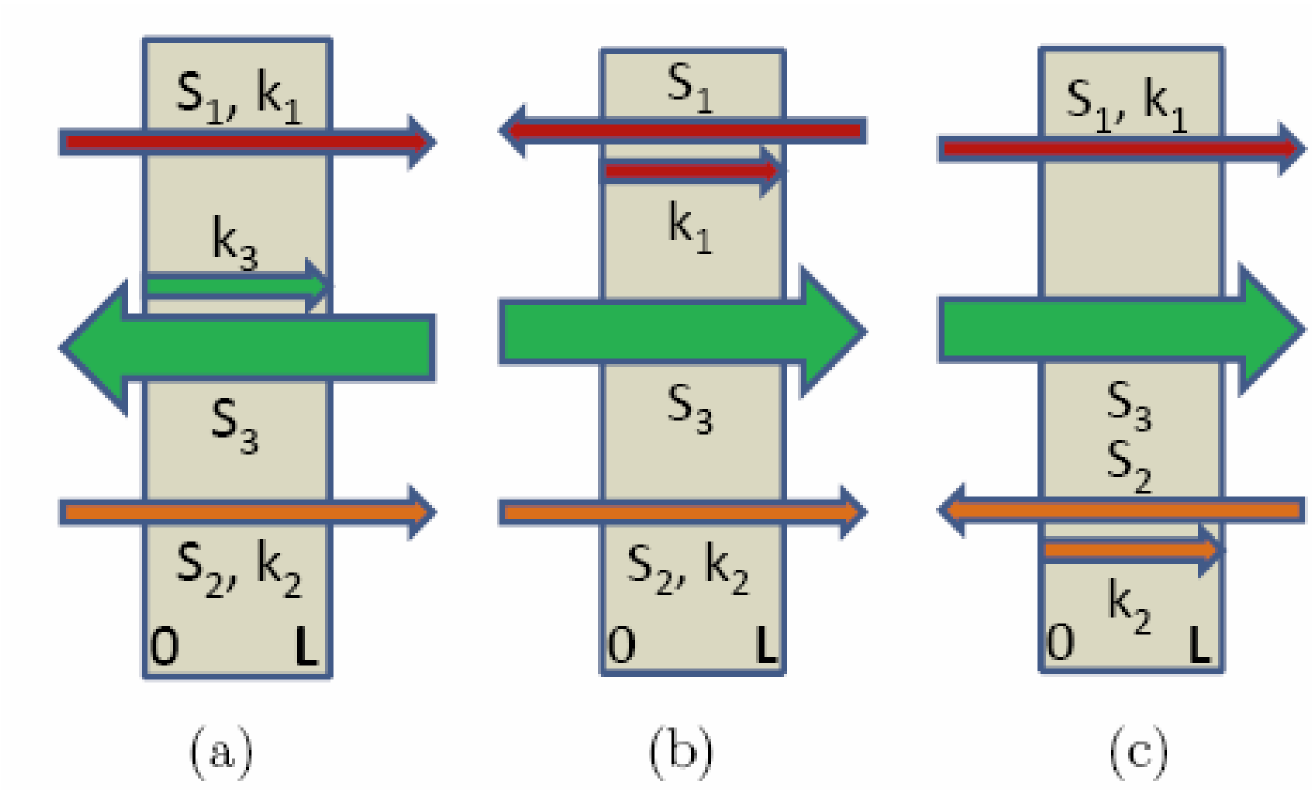

(b) – BW amplifier, (b) and (c) – NLO frequency-converting meta mirrors (NLO sensors)

Popov, Myslivets , ***Proc. SPIE 9157,*** 91573B (2014)

NIMs

$$\boxed{\vec{S} = \frac{c}{4\pi}\vec{E}\times\vec{H}} = \frac{c^2\vec{k}}{4\pi\omega\varepsilon}H^2 = \frac{c^2\vec{k}}{4\pi\omega\mu}E^2$$

$\mu < 0$, $\varepsilon < 0$; $n = -\sqrt{(\varepsilon\mu)}$

Nanoscopic LC ciruits of different geometries.

W. Cai and V. Shalaev, [Optical Metamaterials: Fundamentals and Applications,] Springer, 2009;
https://engineering.purdue.edu/~shalaev/

$$\mu < 0?$$

Different Approach:
Negative SPATIAL Dispersion

Negative Spatial Dispersion and Backward Waves

$$\mathbf{S} = \mathbf{v}_{\boldsymbol{g}}\mathrm{U},\ \mathbf{v}_{\boldsymbol{g}} = \mathrm{grad}_{\mathbf{k}}\omega(\mathbf{k}),$$

$$\mathbf{v}_{\mathrm{g}} = (\mathbf{k}/\mathrm{k})[\partial\omega(\mathrm{k})/\partial\mathrm{k}]\ ,$$

$$\boldsymbol{\partial\omega(\mathrm{k})/\partial\mathrm{k}<0,\ \mathbf{v}_{\mathrm{g}}\uparrow\downarrow\mathbf{k}}$$

V.M. Agranovich, et al, PRB (2004), Phys. Usp (2006).

Spatial Dispersion and Group Velocity

- Free space: $\omega = kc \rightarrow \partial\omega(k)/\partial k = c > 0$;
- Bulk dielectric: $\omega = kv_{ph} \rightarrow \partial\omega(k)/\partial k = v_{ph} > 0$;
- Wave guides: spatially dispersive;
- Optical phonons:

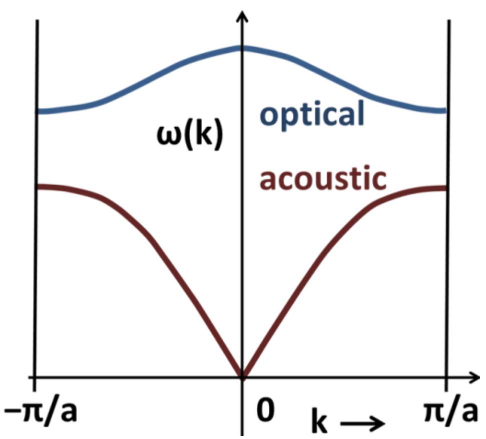

Acoustic phonons exhibit a linear relationship between frequency and phonon wave-vector for long wavelengths. The frequencies of acoustic phonons tend to zero with longer wavelength.

Optical phonons have a non-zero frequency at the Brillouin zone center and show no dispersion near that long wavelength limit.

Diamond: $\omega_v = 1332\ \mathrm{cm}^{-1}$ ($\nu \approx 36.36$ THz),

Calcite $CaCo_3$: $\omega_v = 1086\ \mathrm{cm}^{-1}$

M. I. Shalaev, V.V. Slabko, S.A. Myslivets, A.K. Popov, OL 36, 3861 (2011); *Appl. Phys. A 115, 523-529 (2014)*.

Nanoforest for Extraordinary Backward-wave Nonlinear Optical Processes: SHG and TWM

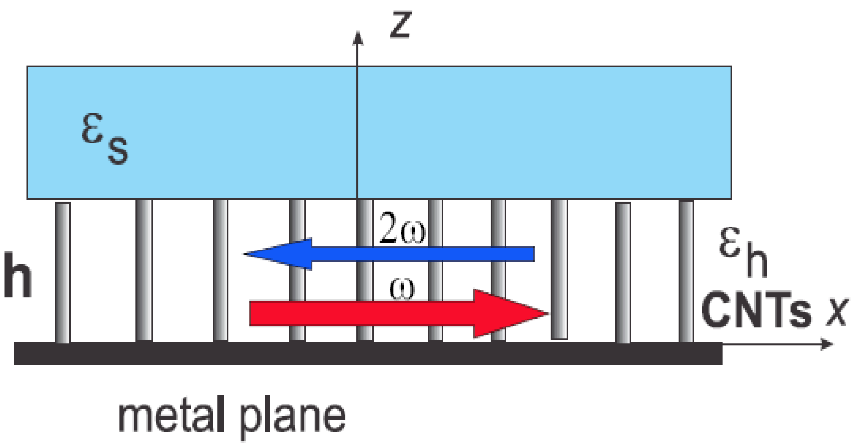

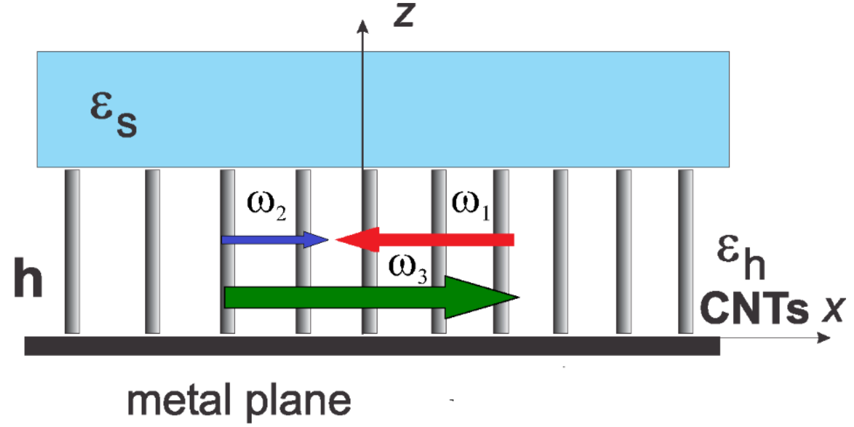

Proof-of-principle Model of the Tailorable Spatial Dispersion and of the MM which Supports the Co-existence of Guided Ordinary and Backward EM Waves with Adjustable Frequencies and Phase and Group Velocities. Phase Matching of Contra-propagating Guided Waves. Greatly Enhanced NLO Generation in the Reflection Direction and Parametric Amplification.

Electromagnetic Properties of Carbon Nanotubes and Dispersion Properties of the Carbon Nanoforest

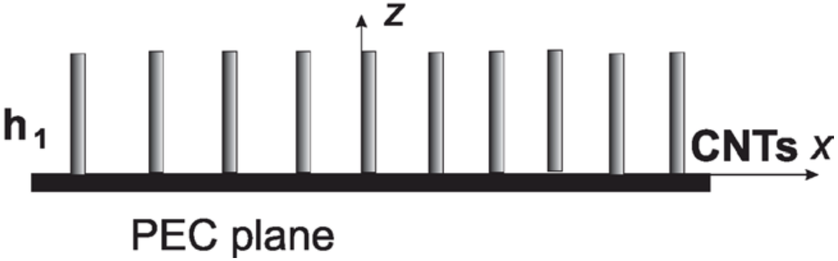

Geometry of free-standing CNTs

Surface conductivity (zigzag CNT):

$$\sigma_{zz} \cong i[2\sqrt{3}e^2\Gamma_0]/[3q\pi\hbar^2(\omega + i\nu)].$$

$$\Gamma_0 = 2.7\ \text{eV},\ r = 3\sqrt{3}qb/2\pi,\ b = 0.142\,\text{nm},\ \tau = 1/\nu$$

Surface impedance per unit length:

$$z_i = \frac{1}{2\pi r\sigma_{zz}} = \frac{\sqrt{3}q\hbar^2\nu}{4e^2\Gamma_0 r} - i\omega\frac{\sqrt{3}q\hbar^2}{4e^2\Gamma_0 r} = R_0 - i\omega L_0.$$

Slepyan, Maksimenko, Lakhtakia, Yevtushenko, Gusakov, PRB **60**, 17136 (1999);
Lindell, Tretyakov, Nikoskinen, Ilvonen, Microw. Opt. Tech. Lett. **31**, 129{133 (2001);

$$\boxed{\frac{\epsilon_{zz}}{\epsilon_0} = 1 - \frac{k_p^2}{k^2 + i\xi k},\quad k_p^2 = \frac{\mu_0}{d^2 L_{\rm cnt}},}$$

k=2π/c, $\xi = \sqrt{\epsilon_0\mu_0}(R_0/L_{\rm cnt})$, $L_{\rm cnt} \simeq L_0$.

For $k_p/k > 1$, $\epsilon_{zz} < 0$.

UNBOUNDED Uniaxial MM:

$$k_\perp^2 = \frac{\epsilon_{zz}}{\epsilon_0}(k^2 - k_z^2)$$

$$\boxed{\mathrm{d}k_\perp^2/\mathrm{d}k^2 < 0,}\quad \text{if } k_z/k > 1 \text{ and } k_p/k > 1$$

All TM modes are backward waves.

Nefedov, PRB **82**, 155423 (2010);
Nefedov, Tretyakov, PRB **84**, 113410 (2011);
Popov, M.I. Shalaev, Myslivets, Slabko, Nefedov, Appl. Phys. A **109**, 835{840 (2012),
Narimanov, PRX **4**, 041014 (2014).

Guided TM Waves

TM waves

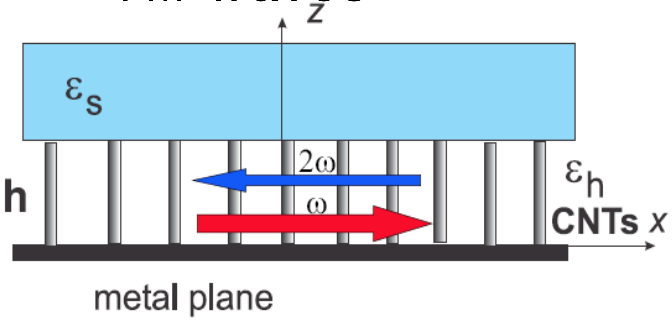

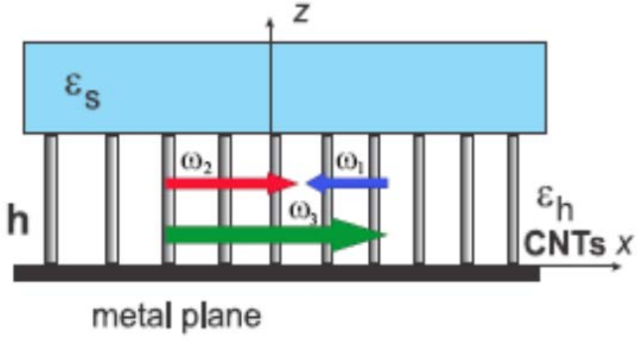

Popov, et.al., Appl. Phys. A 109, 835 (2012),
http://arxiv.org/abs/1602.02497.

Dispersion Equation $k(k_x)$

$$\boxed{k_z \tan(k_z h) = (\epsilon_\perp/\epsilon_s)\sqrt{k_x^2 - k^2\epsilon_s}}$$

$$k_z = \sqrt{\epsilon_\perp[k^2 - (k_x^2/\epsilon_{zz})]}, \quad k=2\pi\omega/c$$

$$\epsilon_{zz} = 1 - k_p^2/(k^2 + i\xi k),\ k_p^2 = \mu_0/(d^2 L_0)$$

Tampered waveguide
formed by two conducting plates:

$$\boxed{k_x^2 = \epsilon_{zz}\left[k^2 - (m\pi/2h)^2\right]}$$

A. K. Popov, I. S. Nefedov, S. A. Myslivets, Hyperbolic carbon nanoforest for phase matching of ordinary and backward electromagnetic waves: second harmonic generation, **ACS Photonics (April, 2017),**
DOI: 10.1021/acsphotonics.7b00146.

Carbon Nanoforest as a Double Domain Ordinary/BW Metamaterial: Phase Matching for SHG

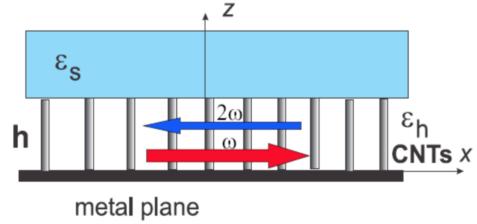

r = 0.82 nm , d = 15 nm, **h = 1.05 μm**. **(h=0.85 μm – the dashed lines)**

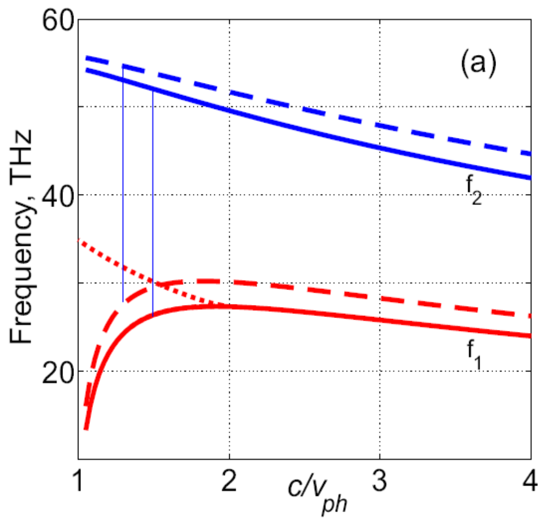

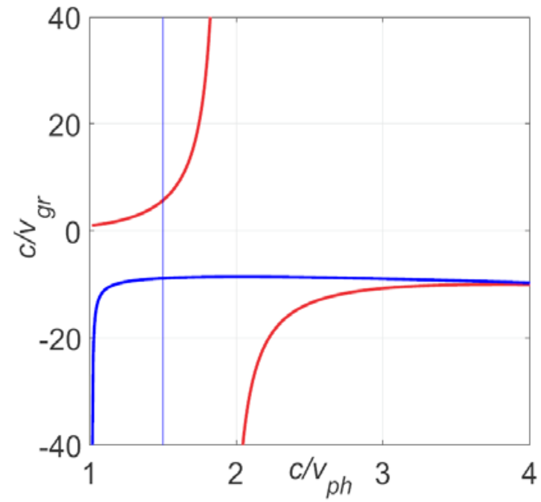

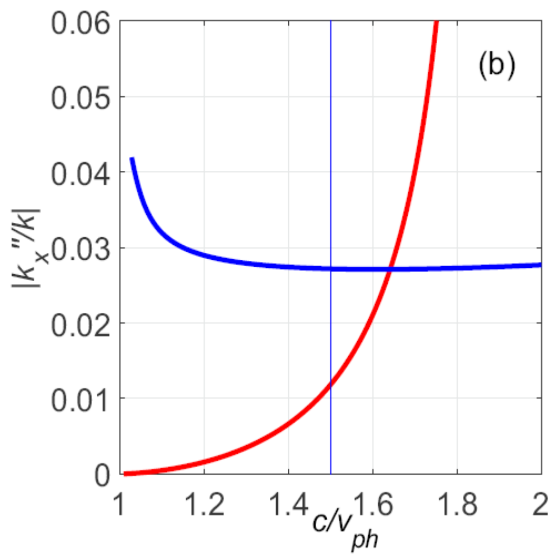

Two EM eigenmodes (EMWs travelling through the nanoforest). Upper: v_g<0, lower: v_g>0 at n_{ph}=1.5 where phase matching occurs.

$v_g = (\mathbf{k}/k)[\partial\omega/\partial k]$.

Attenuation

$c/v_{ph} = k_x'/k_{vac} = n_{ph}$

$f_1 \approx 26.12$ THz, $f_{SH} \approx 52.24$ THz ($\lambda_{1fsp} \approx 12$ μm, $\lambda_{1MM} \approx 8$ μm).

Phase matching of two backward and one ordinary waves: $\boldsymbol{\omega}_1=\boldsymbol{\omega}_3-\boldsymbol{\omega}_2$

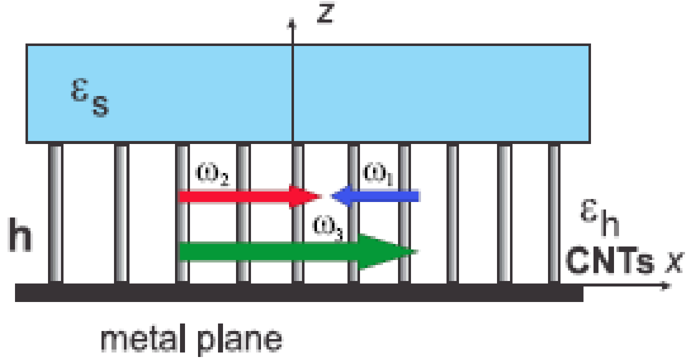

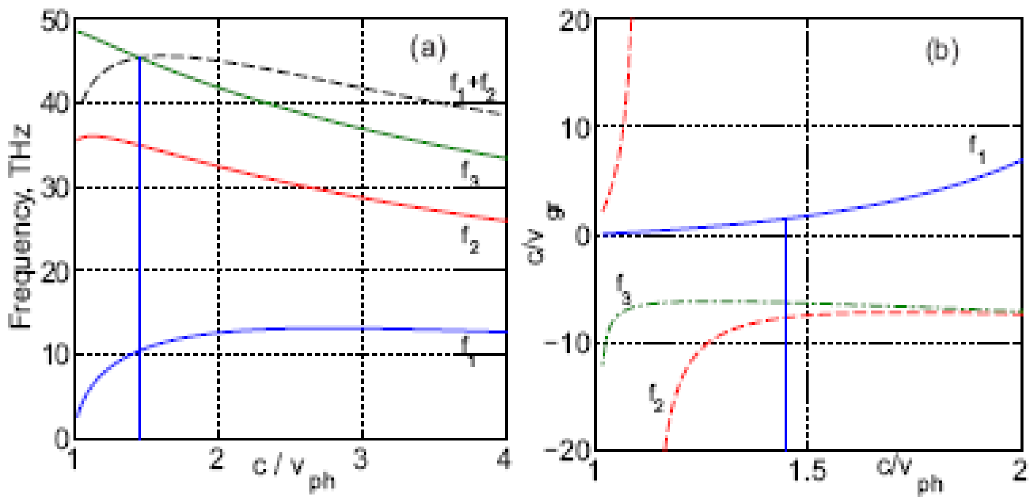

Fig. 2. (a) Dispersion of three lowest modes at $h = 3.5\,\mu$m. The dashed line represents the sum of two lowest modes. (b) Group velocity indices c/v_{gr} for the respective modes.

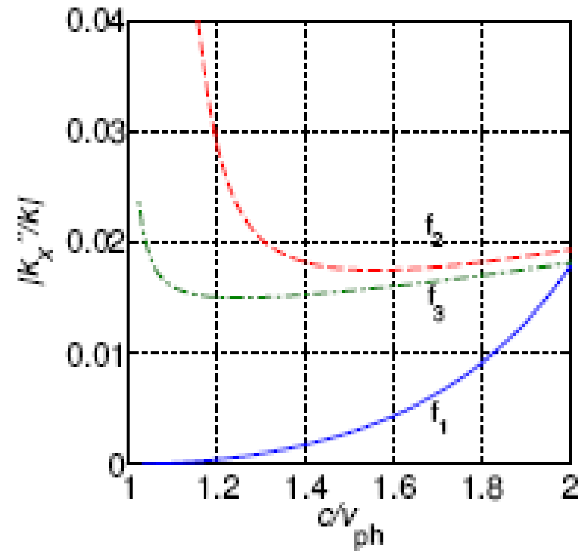

Attenuation

EM Properties of Guided Modes, Numerical Model: h = 3.5 μm, TWM

Table 1

Mode	f, THz	k, 10^5 m^{-1}	$\lvert k_x''/k \rvert$, 10^{-3}	n_g	$\alpha = 2k_x''$, $10^{-2}\mu$m^{-1}	L_a, μm	λ_{vac}, μm	λ_{med}, μm
1	10.43	2.186	2.26	1.45	0.988	2331	28.74	19.86
2	34.95	7.325	17.8	−7.71	2.61	88.2	8.58	5.93
3	45.38	9.511	15.46	−6.29	2.94	78.3	6.61	4.57

L_a : x10 attenuation

BWSHG: Master Equations

$$s_2(\partial a_2/\partial \xi) + (v_1/v_2)\partial a_2/\partial \tau = -igla_1^2 - (\widetilde{\alpha}_2/2d)a_2,$$

$$s_1(\partial a_1/\partial \xi) + \partial a_1/\partial \tau = -i2g^* l a_1^* a_2 - (\widetilde{\alpha}_1/2d)a_1.$$

$$l = v_1 \Delta\tau, \quad \xi = x/l,\ \tau = t/\Delta\tau, d = L/l, \widetilde{\alpha}_i = a_i L, v_i > 0$$

$$F(\tau) = 0.5\left(\tanh\frac{\tau_0 + 1 - \tau}{\delta\tau} - \tanh\frac{\tau_0 - \tau}{\delta\tau}\right)$$

$$\Delta\tau = 10\ \text{ps} \qquad \Delta f \approx 1/\Delta\tau = 0.1\ \text{THz}$$

$$L \approx 40\,\mu\text{m} \quad \alpha_2 L = 2.4,\ \alpha_1 L = 0.41 \qquad \exp(-\alpha_2 L) = 0.1$$

$$l = \Delta\tau v_1 = \Delta\tau c/n_{g,1} = 606\,\mu\text{m}$$

d = L/l ≈ 1/15

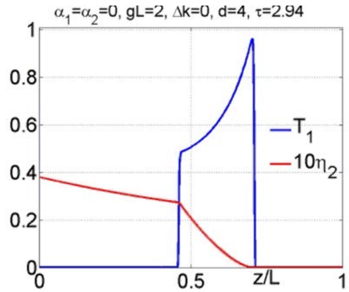

BWSHG vs SHG: Pulse Energy Conversion

BWSHG

Longer slab →

SHG

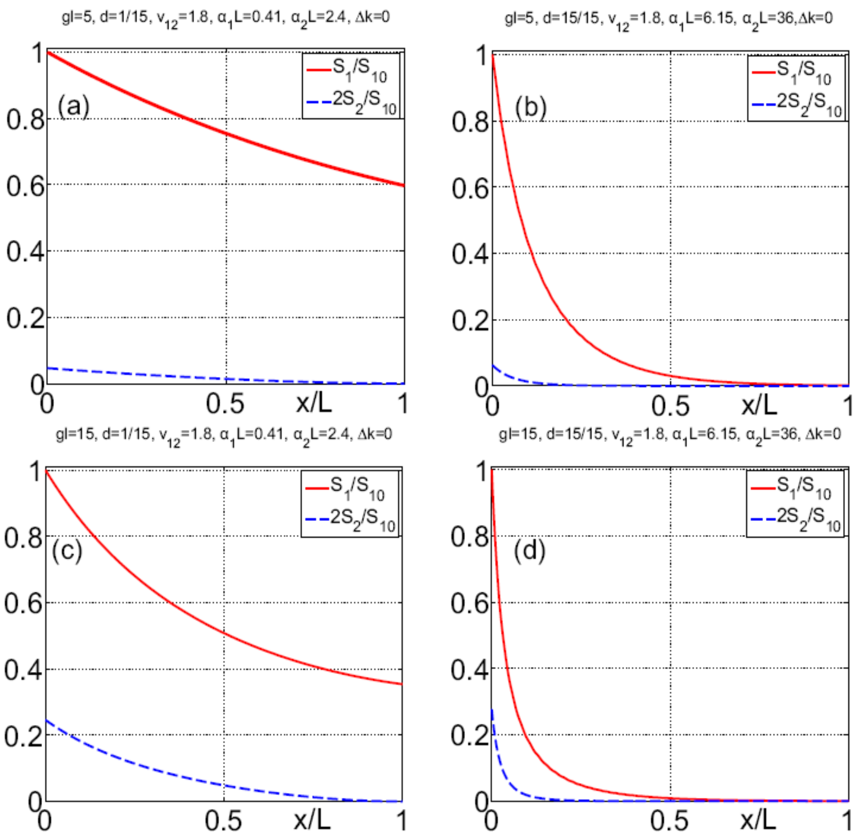

↓ Stronger pump

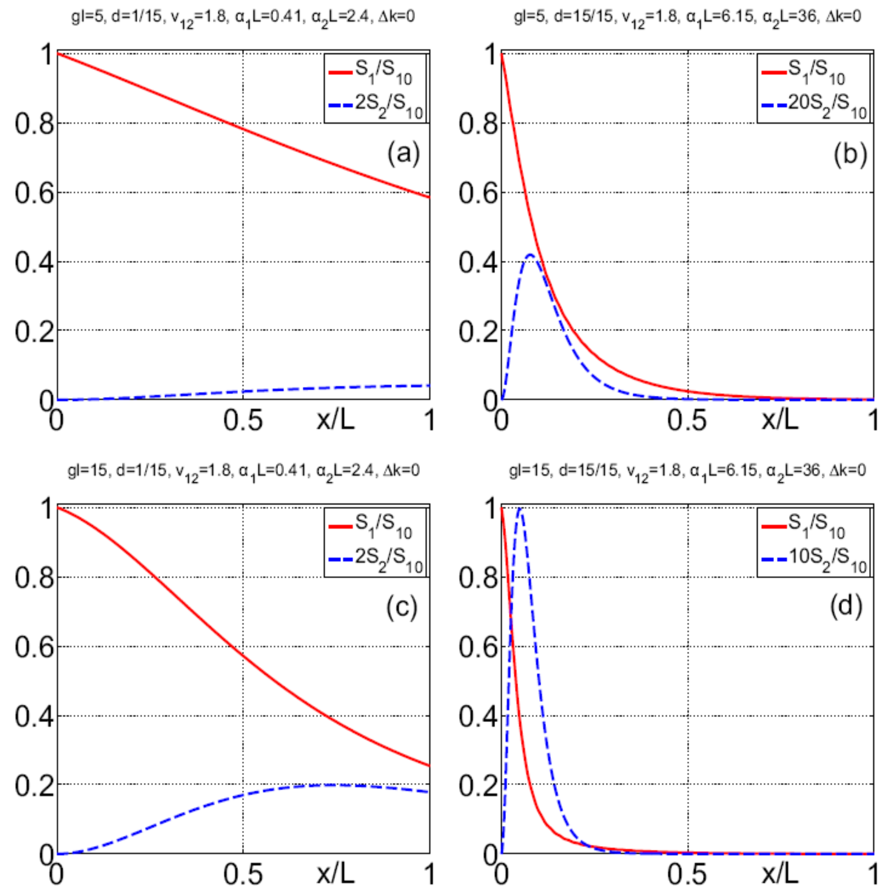

Contra-propagating pulses, **self**-optimization, reduced losses, tailorable pulse shapes

BWTWM: Master Equations and Multi-parameter Dependences

$$s_1 \frac{\partial a_1}{\partial \xi} + \frac{v_3}{v_1} \frac{\partial a_1}{\partial \tau} = -igla_3 a_2^* \exp\left(-i\Delta\widetilde{k}\xi\right) - \frac{\widetilde{\alpha}_1}{2d} a_1,$$

$$s_2 \frac{\partial a_2}{\partial \xi} + \frac{v_3}{v_2} \frac{\partial a_2}{\partial \tau} = -igla_3 a_1^* \exp\left(-i\Delta\widetilde{k}\xi\right) - \frac{\widetilde{\alpha}_2}{2d} a_2,$$

$$s_3 \frac{\partial a_3}{\partial \xi} + \frac{\partial a_3}{\partial \tau} = -ig^* la_1 a_2 \exp\left(-i\Delta\widetilde{k}\xi\right) - \frac{\widetilde{\alpha}_3}{2d} a_3.$$

$$F(\tau) = 0.5 \left(\tanh \frac{\tau_0 + 1 - \tau}{\delta\tau} - \tanh \frac{\tau_0 - \tau}{\delta\tau} \right)$$

Continuous wave seeding signal: $a_{20} = 10^{-5} a_{30}$.

$$\omega_3 = \omega_1 + \omega_2,\ l = v_3 \Delta\tau,\ \xi = x/l,\ \tau = t/\Delta\tau,\ d = L/l,\ \widetilde{\alpha}_j = \alpha_j L$$

$\Delta\tau = 10\,\mathrm{ps}$ $\quad l = \Delta\tau v_{3gr} = \Delta\tau(c/n_{3gr}) = 477\ \mu\mathrm{m}$ $\quad L = L_3 = 78.3\,\mu\mathrm{m}$

BWOPA and NLO Reflectivity vs OPA

BWTWM: resonance gL→π/2

TWM

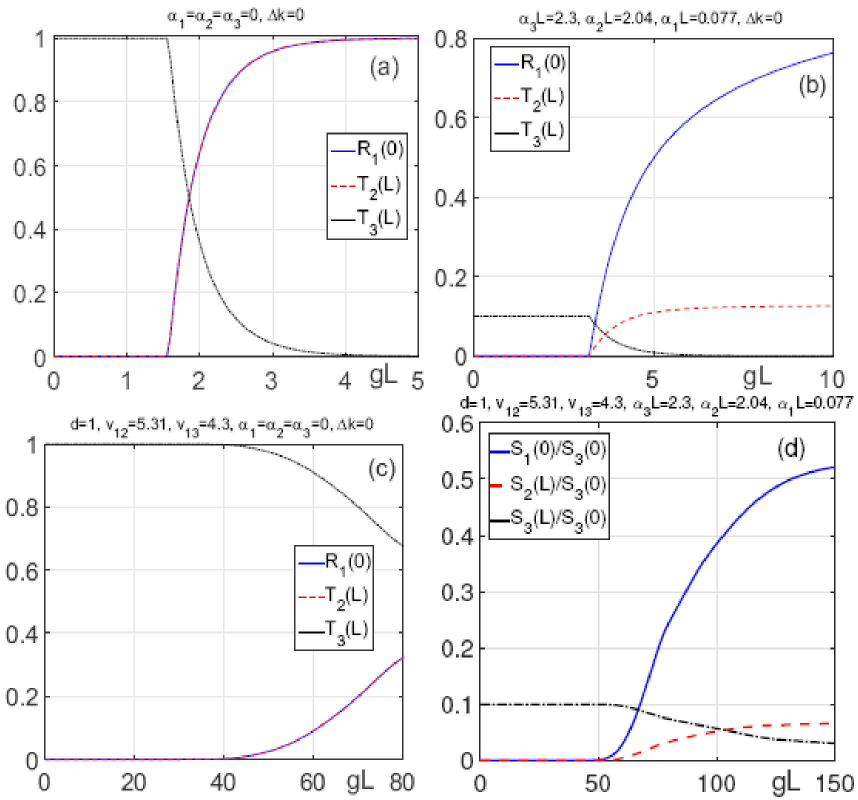

Fig. 4. Optical parametric amplification and frequency-shifting NLO reflectivity vs. intensity of the pump.

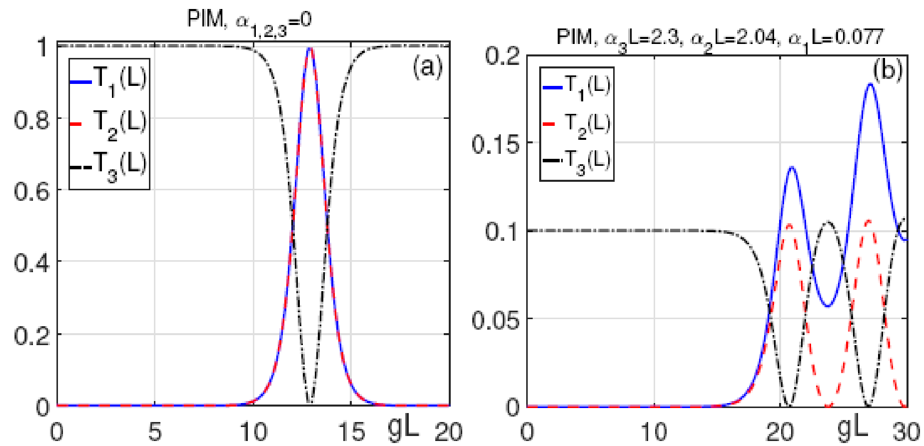

Fig. 6. Output fields vs intensity of the pump for the ordinary, co-propagating coupling scheme. All other parameters are the same as in Figs. 4 (a) and (b) respectively.

$$L = L_3 = 78.3\,\mu\mathrm{m},\ \Delta\tau = 10\,\mathrm{ps}$$

$$l = \Delta\tau v_{3gr} = \Delta\tau(c/n_{3gr}) = 477\ \mu\mathrm{m},$$

(a) and (b): $L/l \approx 1/6$; (c) and (d): $\Delta\tau = (10/6)$ ps.
Effects of the group velocity dispersion and transients.

z = 0, contra-propagating entangled photons

$\mathbf{S_{1,2} \propto 1/\cos^2(gL)}$

$g \propto \chi^{(2)} E_3$

$\mathbf{S_{1,2} \propto \exp(gz)}$

Extraordinary Transient Processes in TWM: Pulse Delay and Pulse Shape Changes

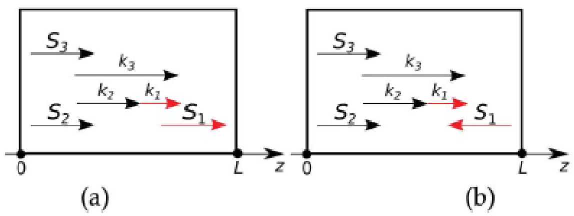

Fig. 1. Two alternative coupling options are (a) co-propagating waves and (b) contra-propagating signal and BW idler waves. Here, $\vec{k}_j$ are wave vectors and $\vec{S}_j$ are Poynting vectors.

z = 0, $S_{1,2} \propto 1/\cos^2(gL)$ $\quad g \propto \chi^{(2)}E_3 \quad$ $\mathbf{gL \to \pi/2}$

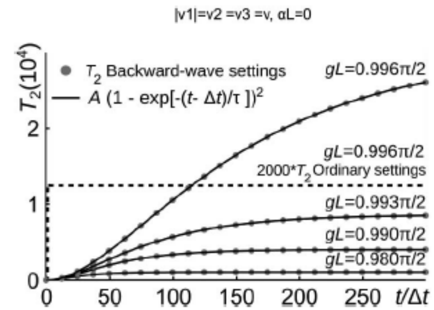

Fig. 3. Dependence of the transient OPA on the intensity of the pump field. The dashed line shows the TWM of co-propagating waves. Points correspond to ordinary signal and contra-propagating idler. The solid lines depict approximation of the transient OPA by the function $T_2(t) = A\{1 - \exp[-(t - \Delta t)/\tau]\}^2$. $-v_1 = v_2 = v_3 = v$, $\alpha_j = 0$.

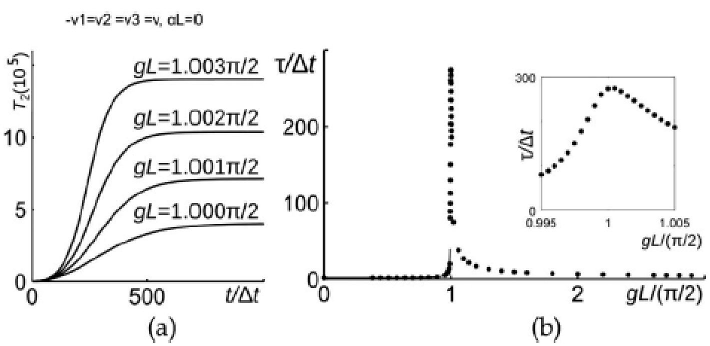

Fig. 4. (a) Shape of the signal forefront in transparent material at pump intensities above the critical input value $gL = \pi/2$. (b) Dependence of the transient period τ on the maximum intensity of the pump field. $-v_1 = v_2 = v_3 = v$, $\alpha_j = 0$.

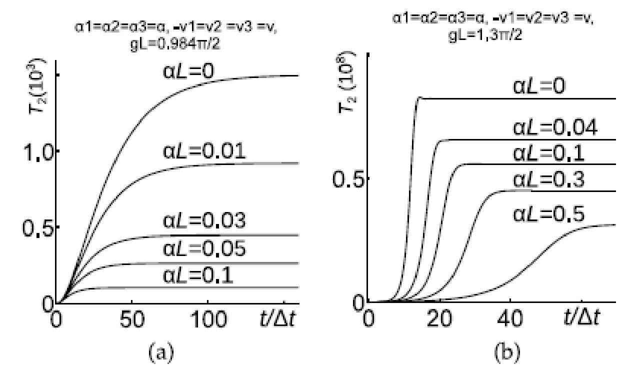

Fig. 5. Effect of absorption on the transient OPA for two different intensities of the pump field. $-v_1 = v_2 = v_3 = v$. $\alpha_1 = \alpha_2 = \alpha_3 = \alpha$. (a) $gL = 0.984\pi/2$. (b) $gL = 1.3\pi/2$.

V. V. Slabko, A. K. Popov, V. A. Tkachenko, and S. A. Myslivets, ***Opt. Lett.*** **41**, 3976--3979 (**2016**).

Conclusions

- The possibility is shown to engineer the metamaterials that enable the co-existence of a spectrum of the optical surface wave-guided electromagnetic waves with different frequencies which propagate in the *opposite* directions while having equal and *co-directed* phase velocities. Phase-matching is the requirement of a paramount importance in coherent nonlinear optics.

- Backward-wave second harmonic generation and three-wave mixing of ordinary and backward electromagnetic waves in a pulsed regime is investigated in such metamaterials. It is shown that the opposite direction of the phase velocity and the energy flux in the backward waves gives rise to *extraordinary* transient processes in the *greatly enhanced* optical parametric amplification and frequency up and down shifting nonlinear reflectivity.

- It is shown that properties of second harmonic generation and three-wave mixingin ordinary and backward-wave settings are fundamentally different. In the latter case, metaslab serves as microscopic frequency-shifting nonlinear-optical mirror which properties can be all-optically controlled.

- The width and shape of the transmitted fundamental, generated and amplified pulses depend on the ratio of pulse length to the metaslab thickness and can be controlled by changing intensity and width of the input pulses.

- Applications in photonics such as novel concepts for creation of ultra-compact, chip-compatible photonic devices with unparalleled capabilities are discussed.

Proof-of-principle Model was developed, investigations and numerical simulations were carried out of the MM which supports the co-existance and the tailorable dispersion of guided backward and forward EM Modes with adjustable phase and group velocities. The investigations proved the possibilities of realization of extraordinary coherent NLO propagation processes and engineering of ultraminiature photonic devices with unparalleled operation properties.

Open Questions:

- **Metamaterials made of low–loss transparent conducting ceramics;**
- **Different shape of the nanostructures, different host and boundary dielectric and nonlinear materials, dynamic control of the dispersion;**
- **NLO coupling of the TE and TM modes;**
- **Operation properties of the corresponding photonic devices, such as photon sources, amplifiers, frequency and propagation direction convertors, modulation and pulse shape control.**

Guler, U. ; Zemlyanov, D.; Kim, J.; Wang, Z.; Chandrasekar, R.; Meng, X.; Stach, E.; Kildishev, A. V.; Shalaev, V. M.; Boltasseva, A. Plasmonics: **Plasmonic Titanium Nitride Nanostructures** via Nitridation of Nanopatterned Titanium Dioxide. *Adv. Opt. Mater.* 2017, *5*, 1600717.

Acknowledgements

Thanks to S. Myslivets, V. Slabko, V. Tkachenko, I. Nefedov, V. Shalaev
for collaboration and inspiring inputs.

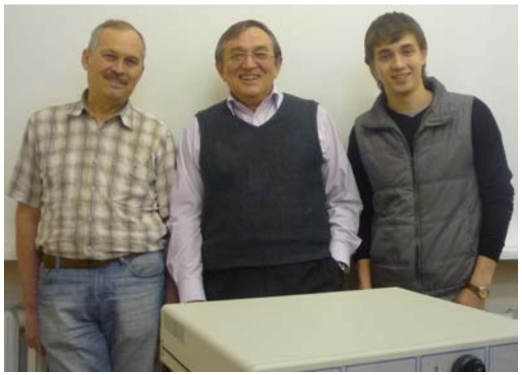

This material is based upon work supported in part by the U. S. Army Research Laboratory and the U. S. Army Research Office under grant number W911NF-14-1-0619.

Published in

A. K. Popov, I. S. Nefedov, and S. A. Myslivets, ``Phase-matched backward-wave second harmonic generation in a hyperbolic carbon nanoforest,'' **http://arxiv.org/abs/1602.02497**.

V. V. Slabko, A. K. Popov, V. A. Tkachenko, and S. A. Myslivets, ``Three-wave mixing of ordinary and backward electromagnetic waves: extraordinary transients,” ***Optics Letters*** **41**, 3976--3979 (**2016**).

A. K. Popov and S. A. Myslivets, ``Nonlinear-optical frequency-doubling meta-reflector: pulsed regime,'' ***Appl. Phys.*** **A 122** (1), 1--6, (**2016**), DOI 10.1007/s00339-015-9534-0.

A. K. Popov and S. A. Myslivets, ``Second harmonic generation and pulse shaping in positively and negatively spatially dispersive nanowaveguides: comparative analysis,'' ***J. Opt. Quant. Electron.*** **48**(2), 1--10 (**2016**), DOI: 10.1007/s11082-016-0416-2.

A. K. Popov, I. S. Nefedov, S. A. Myslivets, ``Hyperbolic carbon nanoforest for phase matching of ordinary and backward electromagnetic waves: second harmonic generation,'' ***ACS Photonics*** (**April, 2017**), DOI: 10.1021/acsphotonics.7b00146.

THANK YOU FOR ATTENTION